ASSIMILATION OF REMOTELY SENSED SOIL MOISTURE INTO HYDROLOGICAL MODEL: A CASE STUDY OF MAHANADI BASIN, INDIA

S. S. Behera[a]*, B. R. Nikam[b], M. S. Babel[c]

[a]M.Engg., Asian Institute of Technology, Thailand (* corresponding author: ssbehera1@gmail.com)
[b]Scientist/Engineer 'SE', Indian Institute of Remote Sensing-ISRO, India (bhaskarnikam@iirs.gov.in)
[c]Professor, Asian Institute of Technology, Thailand(msbabel@ait.asia)

KEYWORDS:*Data Assimilation, parameter sensitivity, Kalman Filter, VIC*

ABSTRACT: Soil moisture is an important hydrologic state variable. Accurate knowledge of the spatial distribution and temporal variation of soil moisture would provide insight into larger-scale hydrological processes and would serve as good land surface moisture initialization states in fully coupled climate system models for improved seasonal-to-inter annual climatological and hydrological prediction. In recent years, air- and space-borne remote sensing campaigns have successfully demonstrated the use of passive microwave remote sensing to map top layer soil moisture at various spatial scales. Data assimilation offers a means to combine the advantages of remote sensing data with the physical based models. Data assimilation technique provides the best analysis estimators by merging the strengths of modelled state and satellite derived observations to achieve higher accuracy and continuous improvement in forecasts. In this study root zone (0–1 m below the ground surface) soil moisture distributions were estimated across the Mahanadi basin, India by assimilating near-surface soil moisture data from the Advanced Microwave Scanning Radiometer for Earth observation science (AMSR-E) with a Kalman filter (KF) data assimilation technique coupled with a Variable Infiltration Capacity (VIC) land surface model.

VIC model was setup for entire Mahanadi basin. The input parameters were derived using different geo-spatial data sources e.g. IMD gridded daily rainfall, temperature, wind speed and cloud has been used as meteorological forcings. NBSSLUP soil map and LULC map of ISRO-GBP LULC project for year 2005 were used for generating the soil and vegetation parameters, respectively. The fluxes obtained from VIC have been routed to simulate discharge for the time period of 1995-2010. Validation of calibrated model is done using observed discharge data from different stations and the coefficient of determination, Nash-Sutcliffe model efficiency coefficient and relative error measured in the validation phase (1995-2010) were 0.95, 0.99 and -0.039, respectively. Assimilated variable (soil moisture) is used to generate multilayer soil moisture regime. A dataset (maps) for different hydrological parameters have been generated on a daily basis which can be used as an important initialization variable in large-scale weather forecasts and climatic predictions modeling.

1. INTRODUCTION

Soil moisture (SM) is a critical parameter in the hydrologic cycle, which controls partitioning of the incoming radiation into latent and sensible heat fluxes, and in the partitioning of precipitation into infiltration, surface runoff and evaporation (Georgakakos, 1996). Spatio-temporal distributions of soil moisture status in the root zone across large landscapes provide important input for many agricultural, hydrological, and meteorological applications (Hanson et al., 1999). Soil moisture varies both in space and time because of spatio-temporal variations in precipitation, soil properties, topographic features, vegetation characteristics and human interventions. Given the importance of soil moisture in Earth system processes, a large amount of research has been devoted to the estimation of this variable at large spatial scale through satellite remote sensing. The first large-scale soil moisture satellite validation program for the Advanced Microwave Scanning Radiometer (AMSR-E) on the Aqua satellite helped to establish several moderate-resolution watershed networks, resulting in a specially designed suite of landscapes for validation (Jackson et al., 2010).Another fundamentally different way to obtain information on the surface SM content is by the application of physically-based spatially distributed land surface models (LSMs). These models simulate processes related to the water and energy balance at the land surface.

Even though both remote sensing and hydrologic modeling are very useful for the estimation of spatially distributed SM, their estimates remain prone to a significant amount of uncertainty and errors (Choudhury et al., 1979; Wang et al., 1983; Pauwels et al., 2001; Wigneron et al., 2004; Panciera et al., 2009; Sabater et al., 2011; Al Bitar et al., 2012; Leroux et al., 2013; Rahmoune et al., 2013; Parrens et al., 2014; Martens et al., 2015). However, by combining hydrologic model predictions with remote sensing observations, improved estimates of soil moisture can be expected at large scales (Lahoz and De Lannoy, 2014). Several studies have shown how improvements in antecedent soil moisture conditions after assimilating microwave remote sensing observations may impact the forecasting of runoff (Brocca et al., 2010, 2012; Draper et al., 2011; Matgen et al., 2012; Pauwels et al., 2002; Pauwels et al., 2001). However, these studies were mainly focused toward active sensors (e.g. ERS and ASCAT) and predictions for small basins. The assimilation of global satellite SM retrievals into hydrologic models presents a

number of challenges. As noted by Wood et al. (2011), it can be expected that LSMs will be applied at fine spatial resolutions, while the remote sensing products will be delivered at significantly coarser spatial resolutions. Either the data assimilation algorithm will have to take into account this spatial mismatch (Sahoo et al., 2013), or the satellite products will have to be pre-processed so their spatial resolution matches the spatial resolution of the hydrologic model (Merlin et al., 2010; Verhoest et al., 2015). Other reasons may relate to approximations and shortcomings in both the retrieval algorithms and land surface models (De Lannoy et al., 2007). However, mitigating these climatologic differences between model simulations and observations of SM is necessary for successful data assimilation (Reichle and Koster, 2004; De Lannoy et al., 2007; Kumar et al., 2012).

Studies have been conducted on improving assessment of profile soil moisture with the help of field based surface soil moisture observations and remotely sensed surface moisture data and it has been concluded that the most promising approach to the problem of profile soil moisture estimation was the integration of remote sensing and computational modeling. (Kostov and Jackson, 1993; Entekhabi et al., 1994). Houser et al. (1998) studied the use of 4-D-Var data assimilation methods in a macroscale land hydrology model to generate root zone moisture fields on regular space and time intervals. Walker et al. (2001) explored the effects of observation depth and update interval on soil moisture profile retrieval and made a comparison of two commonly used assimilation techniques (i.e., direct insertion and Kalman Filter) using synthetic data. They concluded that Kalman Filter (KF) assimilation scheme is superior to the direct insertion assimilation scheme. Profile retrieval was unsuccessful for direct insertion using the surface node alone; observations over some nonzero depth were required. The superiority of the KF lies in its ability to adjust the entire profile, while direct insertion can only alter the profile within the observation depth. On the contrary, Heathman et al. (2003) investigated profile soil water content using direct data assimilation in the root zone water quality model at four field sites in the LittleWashita (LW) River Experimental Watershed during SGP97, and found that direct insertion assimilation improved model estimates down to a depth of 0.30 m at all the sites considered in their study, and no significant improvement in soil water estimates below the 0.30-m depth. Crosson et al. (2002) applied the KF based method for assimilating remotely sensed (ESTAR-based, during SGP97) soil moisture estimates in a point-scale testing scheme and found that even in the presence of highly inaccurate rainfall the model results in good agreement with observed soil moisture.

Generally, data assimilation is used in conjunction with a soil–vegetation–atmosphere transfer (SVAT) model, also known as LSM. The estimation of soil moisture and energy–mass exchange is simulated using SVAT. The accuracy of SVAT models is usually restricted by unreliable estimates of soil moisture (Koster and Milly, 1997). The model can be treated as a stand-alone program, which communicates with the filter through its input and output files. The filter provides a set of random initial conditions, parameters, and forcing variables to the land surface model. In turn, the model derives a time dependent state vector that is passed to the filtering algorithm. This modularity makes it possible to use nearly any land surface model in a data assimilation procedure based on KF. The most frequently used SVAT models with data assimilation are the NOAH model (Chen et al., 1996), Variable Infiltration Capacity (VIC) model (Liang et al., 1996), Mosaic model (Koster and Suarez, 1996), and Common Land Model (CLM; Dai et al., 2003). The SVAT models typically include a thin surface soil layer and one or more, thicker root zone layers and estimate soil moisture of each soil layer at the land–atmosphere boundary and the interfaces between the soil layers. The SVAT models run typically in an uncoupled fashion using a number of generic tools to manage the input and output data. From the vadose zone hydrology perspective at the landscape scale or larger, there is a need for simple and robust integration of surface remote sensing information into a dynamic soil water model in a distributed computing platform (e.g., GIS) to improve the simulation of soil moisture. Hellweger and Maidment (1999) automated a procedure to define and connect hydrologic elements in ARC/INFO and ArcView and write the results to an ASCII file that is readable by the Hydrologic Engineering Center's Hydrologic Modeling System (HEC-HMS).

In this study we have used the modeling capability of Geospatial tools to apply a simple sequential data assimilation (i.e. Kalman Filter) approach in conjunction with a numerically robust Variable Infiltration Capacity (VIC) land surface model (Liang et al., 1994; Liang et al., 1996; Liang et al., 1999) that incorporates remotely sensed surface soil moisture observations (from a passive microwave remote sensor, AMSR-E) to estimate the soil moisture profile. This has the advantage of combining the spatio-temporal continuity of the model prediction with intermittent input of remotely sensed observations in a geographically distributed framework to improve the soil moisture estimation and minimize model and parameter uncertainties using the data assimilation protocol.

2. STUDY AREA AND DATA USED

A river basin at appropriate scale is generally the most logical geographical unit of hydrological analysis and water resources management. The 1,41,589km^2 Mahanadi River basin (Figure 1),encompassed within geographical co-ordinates of 80°28' to 86°43' East longitudes and 19°08' to 23°32' North latitudes, covering major parts of Odisha, Chhattisgarh, small portions of Madhya Pradesh, Maharashtra and Jharkhand states of India, has been selected as

the study area. The average annual discharge at basin outlet, Kendrapada, is 2,119 m^3/s, with a maximum of 56,700 m^3/s during the summer monsoon. Minimum discharge is 759 m^3/s and it occurs during the months October through June. The maximum precipitation in the basin is usually observed in the month of July, August and first half of September. Normal annual rainfall of the basin is 1360 mm (16% CV) of which about 86% i.e. 1170 mm occurs during the monsoon season (15% CV) from June to September (Rao, 1993). In the winter the mean daily minimum temperature varies from 4°C to 12°C. The month of May is the hottest month, in which the mean daily maximum temperature varies from 42°C to 45.5°C.

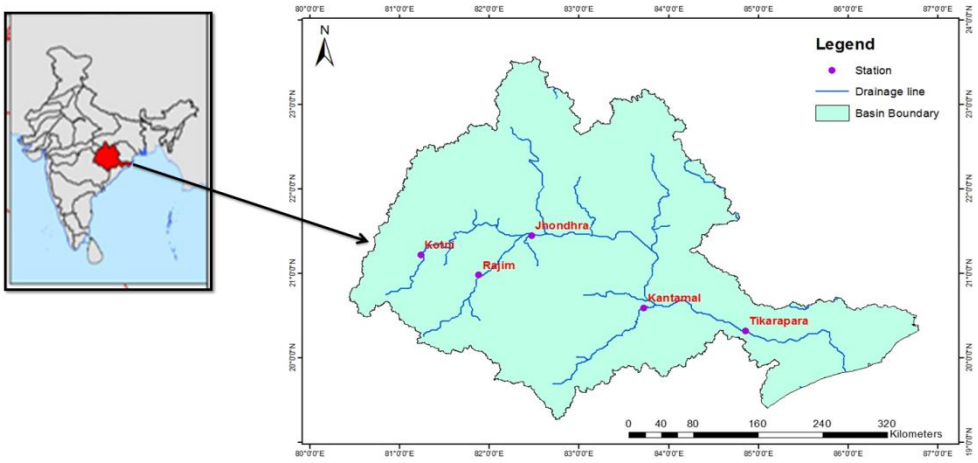

Figure 1: Study Area (Mahanadi River Basin)

An interpolated 0.25°×0.25° gridded daily rainfall dataset developed by India Meteorological Department (IMD) Pune was used to derive daily rainfall in mm over the basin. The daily average wind speed and cloud cover data was rasterized and utilized for the present study. Observed river discharge data of Mahanadi Basin was collected from India-WRIS website and used for model calibration and validation of the results. Shuttle Radar Topographic Mission (SRTM) Digital elevation model (DEM), available at 3 arc seconds having a spatial resolution of 90m, was used in the study to prepare inputs like average elevation in each model grid, slope, basin delineation, elevation bands, flow direction etc. National Bureau of soil survey and Landuse Planning (NBSSLUP)generated soil map and LULC map of ISRO-GBP LULC project entitled "Land Use Land Cover Dynamics and Human Dimension in Indian River Basins" at 1:2,50,000 scale were used for generating the soil and vegetation parameters respectively. The major soil types found in the basin include red and yellow soils, mixed red and black soils (laterite soils). Sandy loam (38.3%), loam (25.53%), loamy sand (19.15%), light and heavy clay (6.38%) and sand clay loam (4.26%) are the predominant textures on the soil surface as given in Figure 2 (a). Land use and land cover (LULC) is dominated by cropland (56.36%), rice being the major crop as given in Figure 2 (b). Daily soil moisture product of AMSR-E for the month of August 2010 has been used in the present study for assimilation in VIC and validation of model results with respect to soil moisture.

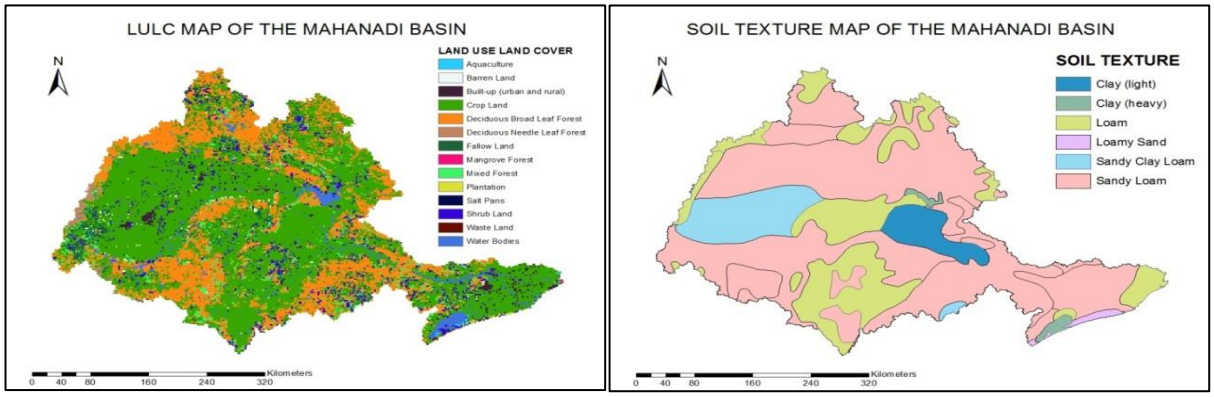

a) Land Use Land Cover (Source: IGBP) b) Soil Texture (Source: NBSSLUP)

Figure 2: a)Land Use Land Cover Map and b) Soil Texture Map of the Mahanadi Basin

3. METHODOLOGY

The methodology is broadly divided into two main steps a) Setting up of the VIC model, model calibration/validation and modeling the hydrological components of the basin; b) Assimilation of satellite derived soil moisture data into the VIC model using data assimilation techniques and generating the scenario. In this

research VIC-3L model (Liang et al., 1994) which solves both water balance and energy balancehas been implemented. This model accounts for the heterogeneity of the surface such as subgrid variability of vegetation classes, soil moisture storage capacity as it divides the whole study area into number of grids. Study area has been divided into square grids of 25km resolution. At first model was set up and run in the water balance mode. The fluxes obtained from VIC have been routed to simulate the discharge for the time period of 1995-2010. Kalman Filtering Data Assimilation technique has been implemented for the year 2010 in this study to improve the model forecasts of soil moisture.

3.1Methodology for VIC Modeling

3.1.1 VIC Setup

The Variable Infiltration Capacity (VIC-3L) model (Liang et al., 1994, 1996, 1999) is a distributed LSM that accounts for both the water and energy budgets. During the last decades, the VIC model has been widely used in a number of applications (Maurer et al., 2001; Nijssen et al., 2001; Sheffield et al., 2003; Sheffield and Wood, 2008; Dadhwal et al., 2010; Aggarwal et al., 2012; Aggarwal et al., 2013; Nikam et al., 2015; Shiradhonkar et al., 2015; Garg et al., 2016; Garg et al., 2017a, b; Nikam et al. 2017). The grid cell size of VIC can be specified between 1 km and hundreds of kilometers, where each cell can be statistically subdivided into fractions that represent different land cover types. The present study uses a grid resolution of 25km×25km. Associated with each land cover type is a single canopy layer, and three soil layers. The canopy layer determines the interception of precipitation as a function of leaf area index (LAI) according to a biosphere– atmosphere transfer scheme (BATS) (Dickinson et al., 1986). It includes a top thin soil layer to represent quick bare soil evaporation following small rainfall events, a middle soil layer to represent the dynamic response of the soil to rainfall events, and a lower layer to characterize the seasonal soil moisture behaviour (Liang et al. 1994, 1996; Liang and Xie 2001). The first soil layer represents the top 10 cm, whereas the second and third layer depths are variable. The first two layers control the partitioning of precipitation into surface runoff and infiltration, hence, they capture the dynamic response to the infiltrated precipitation. Thereby, diffusion of soil moisture is allowed in case of a wetter second layer. The infiltration capacity i is given by the Variable Infiltration Capacity curve (Zhao et al.,1980):

$$i = \left[1 - (1 - A)^{1/b}\right] i_m \qquad (1)$$

where i_m is the maximum infiltration capacity, A is the fraction of area for which the infiltration is less than i, and b is a shape parameter. The third layer receives moisture from the second layer through gravity drainage, with a hydraulic conductivity given by the Brooks–Corey relationship for unsaturated soils (Brooks and Corey, 1964), and controls the generation of baseflow through a nonlinear recession curve. VIC- 3L explicitly represents the effects of multiple vegetative covers on water and energy budgets. It uses physically based formulations for the calculation of the sensible and latent heat fluxes, and the conceptual ARNO formulation for base flow (Todini, 1996) to simulate runoff generation from the deepest soil layer. It also uses the conceptual surface runoff model with the Philip infiltration formulation that dynamically represents both the saturation and infiltration excess runoff processes in a model grid cell with consideration of subgrid-scale soil heterogeneity (Liang and Xie 2001; Xie et al., 2003) to simulate runoff generation from the upper two soil layers. For a detailed description of the VIC-3L in this paper, readers are referred to Liang and Xie (2001) and Xie et al. (2003).This LSM uses both space-borne sources as well as ground-based inputs. The VIC model comprises of two working modules: VIC Module and Routing Module. The model works at both daily and sub-daily time step. The overall flowchart of methodology for running VIC model is given in Figure 3.

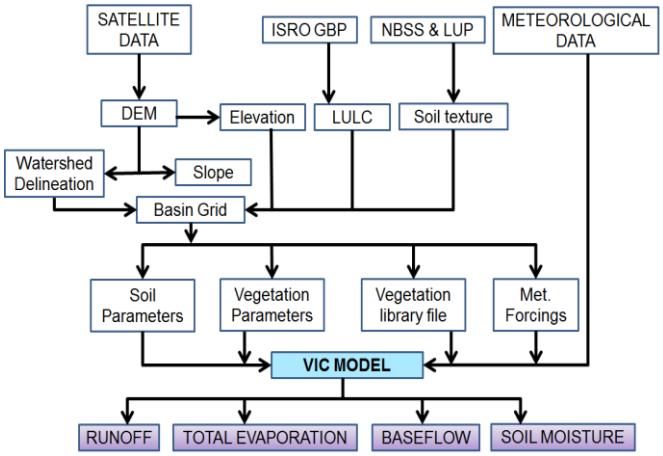

Figure 3:Flowchart for Methodology of Hydrological Modeling Using VIC Model

3.1.2 VIC Model Input Generation

The VIC tool developed by Gupta et al. (2012), as a part of the ISRO-GBP Project on LULC dynamics and impact of human dimensions in Indian River Basins, IIRS Dehradun, was used to prepare the input files. The primary functions performed by the tool are: Data and forcing preparation (Soil parameter preparation, Vegetation parameter preparation), Model execution, Global parameter preparation, Result analysis and Tabular analysis. The inputs for the model are: Terrain (Elevation, Slope, Flow Direction), LU/LC, Vegetation Properties (LAI, Albedo, Root distribution, Canopy Resistance), Soil Properties (Layer-wise physical texture and hydraulic properties) and Meteorological inputs: Daily inputs of Precipitation, Temperature, Wind speed and Cloud cover.

Square grids were generated over the basin covering its entire geographical extent at the resolution of 25km×25km in ArcGIS. The attributes of the grid file include Grid ID, Latitude & Longitude of each grid cell center, Run Grids, Slope(%), Elevation(m), Average Annual Rainfall(mm), Soil Texture of each soil layer. SRTMDEM was used for the preparation of the elevation map and the slope gradient in m/m. Meteorological forcing files were prepared using the IMD gridded data. Four major input files are required to make the VIC model input database namely the Vegetation parameter file, Vegetation Library file, Soil parameter file and Forcing files. The data in these files are stored in the ASCII format. A soil parameter file describes the characteristics of each soil layer for each grid cell. The primary data source to prepare this input was digital soil texture map prepared from NBSS & LUP soil maps (scale-1:2,50,000). The vegetation parameter file describes the vegetative composition of each grid cell. This file cross-indexes each vegetation class (from any land-cover classification scheme) to the classes listed in the vegetation library. To prepare the vegetation parameter file, landuse map was overlaid on the grid map and the number of vegetation classes as well as fraction of grid covered by those classes was extracted. The vegetation library file describes the static parameters associated with each land cover class. The LULC map prepared under ISRO-GBP LULC project has been used for the given study area. The vegetation library file was taken from it. The vegetation library file contains detailed temporal information of biophysical parameters of all the vegetation types influencing water and energy balance process values of these parameters for all the LULC classes were assembled based on Global Land Data Assimilation System database (http://ldas.gsfc.nasa.gov/gldas/GLDASmapveg.php).A global parameter file was generated which contains necessary information to specify the user preferences and the parameters and to include information regarding the number of layers, time step, location of the input and the output files, the modes which are to be activated. The VIC 4.0.6 was compiled using gcc complier on Linux operating system. Global control parameters were modified according to the input characteristics to activate the water balance. VIC source code is executed in the LINUX environment to generate the flux files for each basin grid. These flux files contain surface runoff, evapotranspiration, baseflow, soil moisture etc. produced at that location. The grid based runoff fluxes are routed using a stream flow routing model developed by Lohmann et al. (1996). The inputs files for this routing scheme are flow direction file, the fraction and station files. Above stated input files are prepared using DEM as the primary input. A control file defining user preferences and location of input files will be used to call the routing code in LINUX environment.

3.1.3 VIC model calibration and validation

The daily runoff fluxes were routed to multiple observation stations using VIC routing model proposed by Lohmann et al. (1996) and Lohmann (1998a, b). The simulated discharge at Tikarapara observation station has been used during calibration phase of the model. The primary aim of calibration process was to minimize the difference between simulated and observed hydrological output from the basin, which in present case is the annual and monthly discharge at Tikarapara observation station. The comparison of simulated discharge from VIC with the observed discharge data for the time period not considered during calibration or for stations not considered can hint the success of calibration phase. This comparison is known as validation of the calibration phase. Validation of results has been done at the Jhondra gauging station for the period of 1995-2010. Three performance indicators were selected for model calibration and validation: (i) Relative error, (ii) The Nash– Sutcliffe coefficient (Nash and Sutcliffe, 1970), and (iii) Coefficient of Determination, (R^2).

1) The relative error (Bias; %) between simulated and observed mean annual runoff, which reflects the error of the total monthly or annual flow volume.

$$R.E. = \frac{\left(\overline{Q_m} - \overline{Q_0^t}\right)}{\overline{Q_0^t}} \qquad (2)$$

2) The Nash–Sutcliffe model efficiency coefficient is used to assess the predictive power of hydrological models. It is defined as:

$$N_s = 1 - \frac{\sum_{t=i}^{T}\left(Q_0^t - Q_m^t\right)^2}{\sum_{t=i}^{T}\left(Q_0^t - \bar{Q}_0\right)^2} \qquad (3)$$

where Q_o is the mean of observed discharges, and Q_m is modelled discharge. Q_o^t is observed discharge at time t.Nash–Sutcliffe efficiency can range from $-\infty$ to 1. An efficiency of 1 (E = 1) means that the model perfectly predicts the observations.

3) The Coefficient of Determination is the square of the Pearson's Product Moment Correlation Coefficient (i.e., $R^2 = r^2$) and describes the proportion of total variance in the observed data that can be explained by the model. It ranges from 0.0 (poor model) to 1.0 (perfect model) and is given by:

$$R^2 = \left\{ \frac{\sum_{i=1}^{N}(O_i-\bar{O})(P_i-\bar{P})}{\left[\sum_{i=1}^{N}(O_i-\bar{O})^2\right]^{0.5}\left[\sum_{i=1}^{N}(P_i-\bar{P})^2\right]^{0.5}} \right\} \quad (4)$$

where O and P denotes the observed and predicted discharges, the over-bar denotes the mean for the entire time period of the evaluation.

3.2 Soil Moisture Data Assimilation in VIC

Data assimilation systems are typically designed to merge uncertain predictions from models with incomplete and noisy measurements from an observing system. Assimilation approaches optimally combine model predictions and independent observations in such a manner that the shortcomings of each approach are mutually compensated. Methodology for data assimilation given in the flowchart (Figure 4) focuses mainly on the soil moisture assimilation. The assimilation of AMSR-E daily soil moisture product has been done in the soil parameter file of the VIC input.

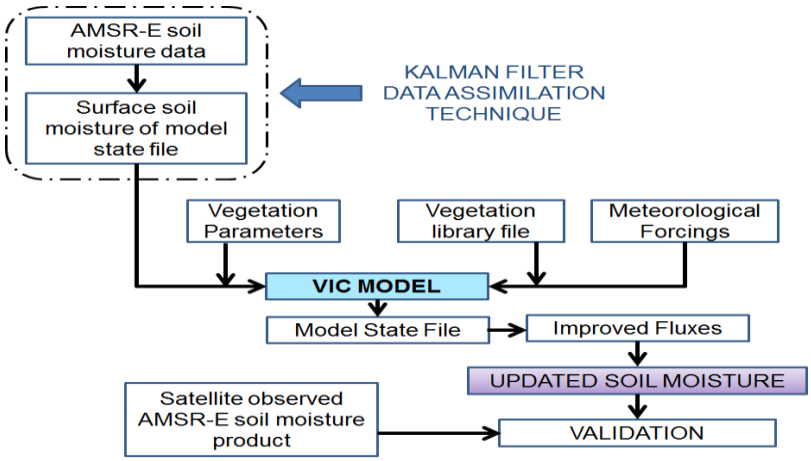

Figure 4: Methodology for Soil Moisture Data Assimilation in VIC Model

VIC model is run in the 'model state' mode a daily time step. Then, the state files were updated after running the model assimilated with the data and then the effects have been observed on the various outputs and on the multi-layer soil moisture regime. Surface soil moisture (1-2cm) observations derived from AMSR-E for the year 2010 has been used for the purpose. Kalman filtering technique has been applied to assimilate AMSR-E soil moisture data for the month of August, 2010 for all the grids of the basin. Kalman gain was calculated for all the run grids in 52×52 matrix samples for 4 times to cover all 208 grids. AMSR-E observed soil moisture data values were multiplied by conversion factor 0.001 to obtain soil moisture in g/cc which was further converted to mm before assimilating into the model.

In this section, the Kalman filter algorithm has been described. The Kalman filter is a recursive algorithm that updates an analysis state from a weighted average of a model prediction and observations of the true state. A successful Kalman filter update will result in the analysis state being a more accurate estimate of the true state than either the model prediction or the observations alone. Furthermore, the Kalman filter algorithm assumes that there exists a linear observation operator H from the state space to the observation space The Kalman filter formulates the background error covariance matrix P^b for the background state as:

$$P^b = X'^b_1 (X'^b_1)^T \quad (5)$$

Where, P^a is the analysis covariance matrix from the previous Kalman filter update step. These covariance matrices P^a and P^b, respectively, describe the uncertainty in the estimated analysis state and the estimated background state. Perturbation from mean for the i^{th} member

$$X'^b_1 = X^b_1 - X^b_i \quad (6)$$

From Eq (7), we see how the Kalman filter update step acts as a weighted average between the model estimate background state X_i^b and the observations Y (i.e. soil moisture measurements) ,based on uncertainties in both, which produces an analysis state X_i^a and its associated covariance matrix P^a. The most common formulation of the Kalman filter update step is: Analysis = Background + Kalman Gain × (Innovation) given by the equation:

$$X^a_i = X^b_i + K\left(Y - H\left(X^b_i\right)\right) \quad (7)$$

$$P^a = P^b(1 - KH) \quad (8)$$

Where the Kalman gain matrix in Eqn. (7) and (8) is defined as

$$K = P^b H^T (H P^b H^T + R)^{-1} \quad (9)$$

where, X_i^a = updated estimate of the analysed state. (n×1 dimension); X_i^b = background Model forecast also referred as the first guess in data assimilation (N×1 dimension); i=1 to N, where N is the number of ensembles; X_1^b or Y = Observations (p×1 dimension & p is the no. of observations) soil moisture measurements; H = Observation operator that converts the states in the model into observation space (p×n dimension); K = Kalman gain that weighs the effect of the observations to the state update (p×n dimension); R= Observation error covariance with dimension (p×p); P^b=Background error covariance

It is observed in Eq. (8) how the KH term acts as a rank correction from the background covariance to the analysis covariance, which can then result in a reduction in the error of subsequent state analyses. By definition, a covariance matrix is positive semi-definite, so it might not be invertible. In order to ensure that the Kalman gain matrix K in Eq. (9) is well-defined, the linear Kalman filter formulation typically assumes observations are independent of each other, which implies that the observation error covariance matrix R is positive definite and of full rank m. The analysis state X_i^a from these two Kalman filter formulations is a unique, unbiased, minimum variance estimate of the true state when the model and the observation operator are linear.

The Background error covariance matrix, Error covariance matrix, Kalman gain matrix and Analysis matrix were generated. Error covariance matrix R is important to eliminate the errors accounted for in the observation data. KF works on the principle of BLUE (Best Linear unbiased Estimator), hence 20% error in AMSR-E soil moisture product has been assumed and for this standard deviation, the Error covariance matrix is estimated same as background matrix. Model state soil moisture is in mm hence we have to convert AMSR-E soil moisture product from g/cc to mm. The observation error covariance matrix is a diagonal matrix of dimension 52×52 generated for all the grids of the entire basin for 31 days. Then the Kalman gain was reckoned for all the grids for the entire month of August. Kalman gain matrix H is identity matrix because model forecasted soil moisture and the same variable's satellite observation has been applied in equation which seems there is no need of conversion factor for state to observation. Analysis matrix gives the updated states of soil moisture. The updated state i.e. after assimilation is of dimension 1×52. The updated soil moisture was again incorporated in state file generated for that particular day by running VIC. It is done by using fraction of vegetation tiles in each grid and the soil moisture was estimated by VIC for respective vegetation fraction in the same grid. Weighted average of each fraction of vegetation and its respective moisture was calculated and then simply by multiplying the analysis i.e. updated soil moisture from KF to each average the new soil moisture was estimated for each fraction of each grid, after which the old state file was replaced by new soil moisture values and new file was generated to run VIC to get new model states i.e. forecasts.

4. RESULTS AND DISCUSSION

The grid based VIC-3L model setup for Mahanadi basin was forced with observed meteorological forcings. Other essential input parameters pertaining to topography, vegetation cover and soil were generated using geo-spatial data sources and/or tools. The model was run in water balance mode for the time period 1995 to 2010. The resultant surface water balance fluxes were used as input for VIC routing model along with other topographical inputs. The routed discharges for different locations were used to evaluate hydrological behaviour of model. The results of model calibration and validation process area described here.

4.1 VIC Model Calibration and Validation

First the model was simulated by considering initial values of calibrating parameters. Keeping the results of the initial iteration as reference, the remaining parameters were increased or decreased until the best match between the observed and simulated discharge was obtained. The best match between simulated and observed discharge was observed for the soil calibration parameters such as *bi*=0.4, *Ds*=0.001, *Ws*= 0.9 for soil zone 0.05, 0.25, 0.70. Soil calibration parameter bi, which defines the shape of the variable infiltration curve, is the most sensitive parameter affecting runoff of the basin followed by *Ws* and *Ds*. The hydrograph of the monthly observed and simulated discharge at Tikarapara station, a gauging station used for model calibration process, after calibration is presented in Figure 5.

In the present study model calibration is done at Tikarapara gauging station which is considered as the main outlet of the Mahanadi Basin and validation of results is done at the Jhondra gauging stations.R^2 value of scatter plot between observed and simulated monthly discharge at Tikarapara gauging station is 0.953 which shows that the model is well calibrated. Essentially, the closer the value of R^2 and N_s is to 1, the more accurate the model is. The more the relative error or bias is closer to 0, indicates less model error or inaccuracy.The R^2 value of scatter plot at Jhondra gauging stations are 0.856 which shows that the model is well validated. Mean annual observed discharge at Tikarapara gauging station is 18105.36 cumec whereas calibrated model simulated mean annual discharge is

18049.49 cumec which shows model is well calibrated to be used for further study. The Nash–Sutcliffe model efficiency coefficient is used to assess the predictive power of hydrological models. The Nash–Sutcliffe model efficiency coefficient between observed and simulated discharge is 0.9979 at Tikarapara gauging station. The R^2 value, Nash-Sutcliffe model efficiency coefficient and Relative error values for monthly and mean monthly simulations at each gauging station are summarised in Table 2 for both the calibration and validation phases of the model. The hydrograph of the monthly observed and simulated discharge at Jhondra station after validation is presented in Figure 6.

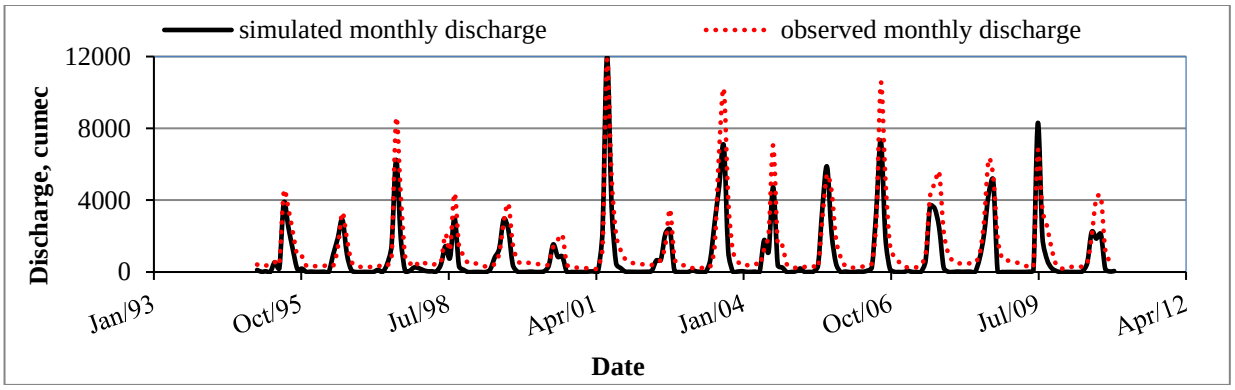

Figure 5: Hydrograph for simulated and observed monthly discharge at Tikarapara (calibration phase)

Table 2: Performance indicators during model calibration and validation

Outlet	Monthly Simulation			Mean Monthly Simulation		
	R^2	N_s	R.E.	R^2	N_s	R.E.
MODEL CALIBRATION PHASE (1995-2010)						
Tikarapara	0.8655	0.9138	-0.0396	0.9527	0.9979	-0.0031
MODEL VALIDATION PHASE (1995-2010)						
Jhondra	0.7691	0.9998	+0.0131	0.8555	0.9933	-0.0265

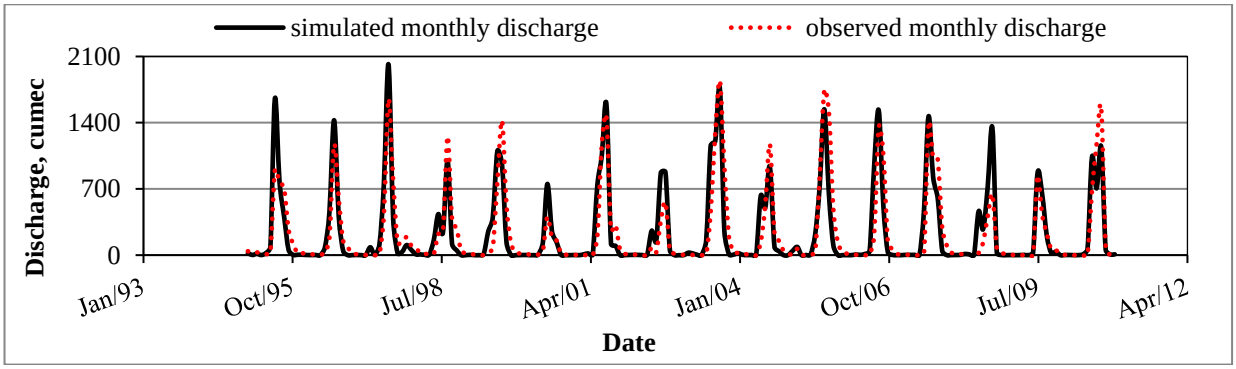

Figure 6: Hydrograph for simulated and observed monthly discharge at Jhondra (validation phase)

4.2 Data Assimilation Results

In this study, the top layer soil moisture estimation from the AMSR-E on the NASA EOS Aqua satellite has been applied to retrieve deep-layer soil moisture as well as other fluxes using the VIC land surface hydrologic model and KF data assimilation technique. Assimilation has been done for the month of August, 2010 for all the grids of the basin.

Results have been compared with rainfall events to check the soil moisture variability and effect of irrigation in the respective grids. Figure 7 is the graphical representation of observed, model simulated and updated estimates of soil moisture for grid number 349, showing the effect precipitation on DA. Considering the satellite data to be true (observation), assimilation has pulled down the modelled state towards observed data and the effect of assimilation continues as long as there is not much influence of rainfall event as shown in Figure 7. With increase in rainfall the assimilated soil moisture is again pulled towards the modelled soil moisture state. Forecasted soil moisture changes

following the rainfall trend but the assimilated soil moisture follows the pattern of water balance. Same results can be observed for all the grids of the basin. Few grids have been selected to show the behaviour of the assimilated soil moisture with respect to modelled and observed.

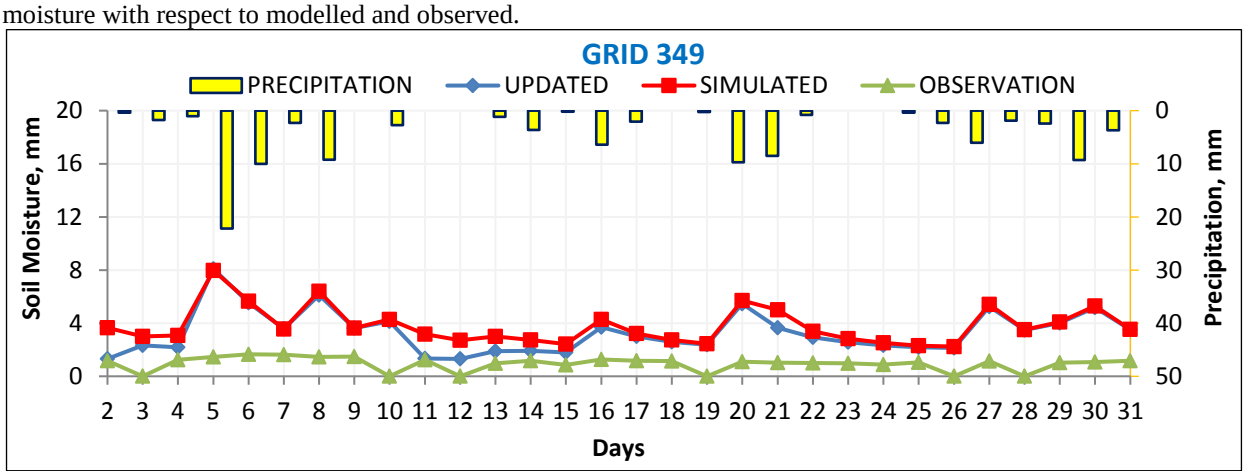

Figure 7: Impact of Data Assimilation on Modelled State Moisture

When there is no rainfall the forecasted moisture continuously decreases whereas assimilated trend may increase or decrease that means the surface irrigation phenomenon is observed well due to assimilation of observed soil moisture in the model. Any of the basin scale hydrological model is setup using virgin conditions and therefore it cannot incorporate irrigation facility which is more of a localized activity. Therefore, in pixels where there is human intervention in terms of water distribution (irrigation), the model fails to predict correct state of model parameters (e.g. soil moisture, evapotranspiration, runoff, etc.).Even satellite observation cannot penetrate to more than 5cm of soil depth and are often obstructed by dense cloud cover and vegetation. Assimilation of observed data merges the advantages of both model and observation to give accurate results.

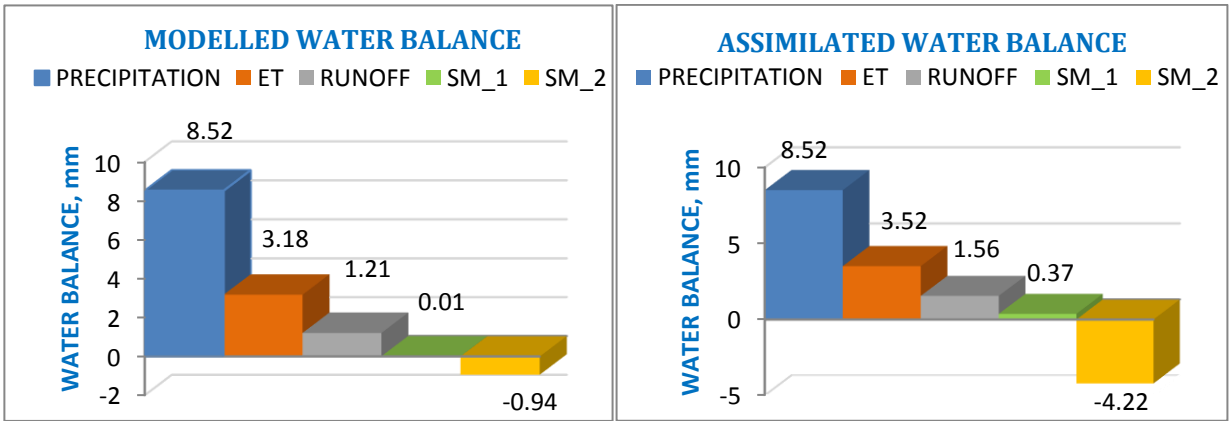

Figure 8: Water budget without(a) and with(b) assimilation

Data assimilation has been performed for the 31 days of August month in three intervals on day 2, 11 and 31 after every 10 days. The first assimilation phase was from day 2 to day 11, second assimilation from day 11 to day 21 and third phase from day 21 to day 31.Day 1 is not considered as for that day only 12.4% of grids had observed soil moisture data. On Day 2, 97% of the grids had available observed data. The difference between soil moisture in layer 1 and layer 2 at the beginning of assimilation phase and at the end of first assimilation phase are -2.65mm and -2.04mm respectively, for the second assimilation i.e. day 11 to 21, are +1.51mm and -6.09mm respectively and for the third assimilation i.e. day 21 to 31 were +0.52mm and -4.27mm respectively. Figure 8 gives a clear idea on the modelled and assimilated water budget. Runoff and ET have increased after assimilation. First and second layer deficit has increased with assimilation. Modelled (without assimilation shown in Figure 8a) and updated (with assimilation shown in figure 8b) soil moisture deficit for the 1st layer are 0.01mm and 0.37mm respectively and for 2nd layer are -0.94 and -4.22 respectively. Here, deficit refers to the difference in soil moisture estimates (mm) of day 2 and day 31 of the chosen assimilation period i.e. August, 2010. It is evident from the present study that satellite observed soil moisture can be assimilated at top layer soil moisture in VIC model using Kalman filter DA approach. The assimilated soil moisture product after being validated using field observed soil moisture data can be used for climatic predictions and weather forecasts as well as agriculture and water management.

5. SUMMARY AND CONCLUSION

Basin hydrological response is a very complicated process which is dominated by parameters including land use, terrain, soil texture and characteristics and soil moisture state. Understanding and quantifying the land parameters is essential for management of water resources. Modeling of hydrological components is an efficient method for doing consistent long-term basin behavioural studies. The problem of competently addressing the uncertainty related to hydrological predictions, even after the development of computationally efficient and advanced modeling, still remains a challenging one. Systematic merging of data from different sources into models by data assimilation technique can give higher accuracy and perpetual improvement in hydrological forecasts. Hydrologic data assimilation technique by coupling the advantages of forecast and the remotely sensed observations can achieve higher accuracy and continuous improvement in hydrological estimates. In the present study it has been envisaged to set up a fully calibrated and validated distributed physical based hydrological VIC model for the Mahanadi River Basin, to estimate runoff, evapotranspiration, baseflow and SM on daily basis. The model is parameterized using traditional observed and remote sensing data. VIC model was forced and run to generate fluxes on a daily basis. As recorded from the water balance analysis of the basin, about 22% of total precipitation received by the basin contributes towards runoff generation. From parameter calibration scheme, it is evident that streamflow was found sensitive to variables like upper and lower soil layer depth, velocity of flow and vegetation parameters. Soil calibration parameter, bi, is the most sensitive parameter affecting runoff of the basin followed by Ws and Ds.

Soil moisture being an essential variable for running water as well as energy balance modes has been selected for data assimilation study. This research demonstrates that a Kalman Filter based DA scheme is able to integrate surface soil moisture observations into a distributed land surface model for Mahanadi Basin in India to provide a more accurate soil moisture estimate particularly at the root zone than modeling alone. Assimilated variable (soil moisture) is utilized to generate multilayer soil moisture regime.An improved data set (maps) for different hydrological parameters has been developed on a daily basis which can be used as input data for other activities.Assimilation improves soil moisture estimates in root zone as well as water balance and provides continuous and consistent soil moisture profile estimates. Kalman filter corrects model-generated soil moisture toward the satellite observation, with the size of the correction dependent on the relative magnitudes of the satellite observation and model errors. It has been shown that with the correct model and observation errors, data assimilation provided more accurate root zone soil moisture estimates. Both spatial (all basin grids) and temporal (daily SM estimates for the entire assimilation period) availability of improved soil moisture dataset at daily time-step is ensured by data assimilation.

REFERENCES

Aggarwal, S.P., Garg, V., Gupta, P.K., Nikam, B.R. & Thakur, P.K. (2012). Climate and LULC change scenarios to study its impact on hydrological regime. International Archives of the Photogrammetry, Remote Sensing and Spatial Information Sciences (ISPRS), XXXIX-B8, 147-152, doi:10.5194/isprsarchives-XXXIX-B8-147-2012.

Aggarwal, S.P., Garg, V., Gupta, P.K., Nikam, B.R., Thakur, P.K. & Roy P.S. (2013). Runoff potential assessment over Indian landmass: A macro-scale hydrological modeling approach. Current Science, 104(7), 950-959.

Al Bitar, A., Leroux, D., Kerr, Y. H., Merlin, O., Richaume, P., Sahoo, A., & Wood, E. F. (2012). Evaluation of SMOS soil moisture products over continental US using the SCAN/SNOTEL network. IEEE Transactions on Geoscience and Remote Sensing, 50(5), 1572-1586.

Bhattacharya, T., Aggarwal, S. P., & Garg, V. (2013) Estimation of Water Balance Components of Chambal River Basin Using a Macroscale Hydrology Model. International Journal of Scientific and Research Publications, 3(2)

Brocca, L., Melone, F., Moramarco, T., Wagner, W., Naeimi, V., Bartalis, Z., & Hasenauer, S. (2010). Improving runoff prediction through the assimilation of the ASCAT soil moisture product. Hydrology and Earth System Sciences, 14(10), 1881.

Brocca, L., Moramarco, T., Melone, F., Wagner, W., Hasenauer, S., & Hahn, S. (2012). Assimilation of surface-and root-zone ASCAT soil moisture products into rainfall–runoff modeling. IEEE Transactions on Geoscience and Remote Sensing, 50(7), 2542-2555.

Brooks, R. H., & Corey, A. T. (1964). Hydraulic properties of porous media and their relation to drainage design. Transactions of the ASAE, 7(1), 26-0028.

Brooks, R., & Corey, T. (1964). HYDRAU Properties of Porous Media. Hydrology Papers, Colorado State University, 3, 1–37.

Chen, F., Mitchell, K., Schaake, J., Xue, Y., Pan, H. L., Koren, V., Betts, A. et al. (1996). Modeling of land surface evaporation by four schemes and comparison with FIFE observations. Journal of Geophysical Research: Atmospheres, 101(D3), 7251-7268.

Choudhury, B. J., Schmugge, T. J., Chang, A., & Newton, R. W. (1979). Effect of surface roughness on the microwave emission from soils. Journal of Geophysical Research: Oceans, 84(C9), 5699-5706.

Crosson, W. L., Laymon, C. A., Inguva, R., & Schamschula, M. P. (2002). Assimilating remote sensing data in a surface flux–soil moisture model. Hydrological Processes, 16(8), 1645-1662.

Dadhwal, V. K., Aggarwal, S. P., & Mishra, N. (2010). Hydrological simulation of Mahanadi river basin and impact of land use/land cover change on surface runoff using a macro scale hydrological model. na.

Dadhwal, V.K., Aggarwal, S.P.,& Misra, N. (2010). Hydrological simulation of Mahanadi River basin and impact of landuse/landcover change on surface runoff using a macro scale hydrological model. In International Society for Photogrammetry and Remote Sensing (ISPRS) TC VII Symposium – 100 years ISPRS (eds. Wagner, W. and Szekely, B.), Vienna, Austria, 5–7 July 2010, ISPRS, vol. XXXVIII, Part 7B, 165–170.

Dai, Y., X. Zeng, R.E. Dickinson, I. Baker, G.B. Bonan, M.G. Bosilovich, A.S. Denning, P.A. Dirmeyer, P.R. Houser, G. Niu, K.W. Oleson, C.A. Schlosser, &Yang,Z.-L. (2003). The Common Land Model (CLM). Bull. Am. Meteorol. Soc. 84:1013–1023.

Das, N. N., & Mohanty, B. P. (2006). Root zone soil moisture assessment using remote sensing and vadose zone modeling. Vadose Zone Journal, 5(1), 296-307.

De Lannoy, G. J., Houser, P. R., Pauwels, V., & Verhoest, N. E. (2007). State and bias estimation for soil moisture profiles by an ensemble Kalman filter: Effect of assimilation depth and frequency. Water resources research, 43(6).

Dickinson, R. E.,Henderson-Sellers, A., Kennedy, P. J., & Wilson, M. F. (1986). Biosphere/atmosphere transfer scheme (BATS) for the NCAR community climate model. Technical report, NCAR.

Draper, C. S., Walker, J. P., Steinle, P. J., De Jeu, R. A., & Holmes, T. R. (2009). An evaluation of AMSR–E derived soil moisture over Australia. Remote Sensing of Environment, 113(4), 703-710.

Draper, C., Mahfouf, J. F., Calvet, J. C., Martin, E., & Wagner, W. (2011). Assimilation of ASCAT near-surface soil moisture into the SIM hydrological model over France. Hydrology and Earth System Sciences, 15(12), 3829.

Entekhabi, D., Nakamura, H., & Njoku, E. G. (1994). Solving the inverse problem for soil moisture and temperature profiles by sequential assimilation of multifrequency remotely sensed observations. *IEEE Transactions on Geoscience and Remote Sensing*, *32*(2), 438-448.

Gao, H., Tang, Q., Shi, X., Zhu, C., Bohn, T. J., Su, F., & Wood, E. F. (2010). Water budget record from Variable Infiltration Capacity (VIC) model.Algorithm Theoretical Basis Document for Terrestrial Water Cycle Data Records.

Garg, V., Aggarwal, S.P., Gupta, P.K., Nikam, B.R., Thakur, P.K., Srivastav, S.K., &Senthil Kumar, A. (2017b) Hydrological impacts of land use land cover change over a large basin. Environmental Earth Sciences, DOI :10.1007/s12665-017-6976-z.

Garg, V., Dhumal, I. R., Nikam, B.R., Thakur, P.K., Aggarwal, S.P., Srivastav, S.K. & Senthil Kumar, A. (2016). Water resources assessment of Godavari river basin, India. In Proceedings of ACRS 2016: 37th Asian Conference on Remote Sensing organized at Colombo, Sri Lanka, during October, 17-21, 2016.

Garg, V., Khwanchanok, A., Gupta, P. K., Aggarwal, S. P., Kiriwongwattana, K., Thakur, P. K., & Nikam, B. R. (2012). Urbanisation Effect on Hydrological Response: A Case Study of Asan River Watershed, India. Journal of Environment and Earth Science, 2(9), 39-50.

Garg, V., Nikam, B.R., Gupta, P.K., Srivastava, A., Aggarwal, S.P. & Srivastav, S.K. (2017a). Impact of LULC change on hydrological regime of Krishna basin. In International Conference on the Status and Future of the World's Large Rivers, organized at New Delhi, India, April 18-21, 2017.

Georgakakos, K.P. (1996). Soil moisture theories and observations (special issue). J. Hydrol. 184:131–152.

Hanson, J.D., K.W. Rojas, & M.J. Schaffer. (1999). Calibrating the root zone water quality model. Agron. J. 91:171–177.

Heathman, G. C., Starks, P. J., Ahuja, L. R., & Jackson, T. J. (2003). Assimilation of surface soil moisture to estimate profile soil water content. Journal of Hydrology, 279(1), 1-17.

Hellweger, F. L., & Maidment, D. R. (1999). Definition and connection of hydrologic elements using geographic data. Journal of Hydrologic Engineering, 4(1), 10-18.

Houser, P. R., Shuttleworth, W. J., Famiglietti, J. S., Gupta, H. V., Syed, K. H., & Goodrich, D. C. (1998). Integration of soil moisture remote sensing and hydrologic modeling using data assimilation. Water Resources Research, 34(12), 3405-3420.

Jackson, T. J., Cosh, M. H., Bindlish, R., Starks, P. J., Bosch, D. D., Seyfried, M., & Du, J. (2010). Validation of advanced microwave scanning radiometer soil moisture products. IEEE Transactions on Geoscience and Remote Sensing, 48(12), 4256-4272.

Kalman, R. E. (1960). A new approach to linear filtering and prediction problems. Journal of basic Engineering, 82(1), 35-45.

Koster, R. D., & Milly, P. C. D. (1997). The interplay between transpiration and runoff formulations in land surface schemes used with atmospheric models. Journal of Climate, 10(7), 1578-1591.

Koster, R. D., & Suarez, M. J. (1996). Energy and water balance calculations in the Mosaic LSM. National Aeronautics and Space Administration, Goddard Space Flight Center, Laboratory for Atmospheres, Data Assimilation Office: Laboratory for Hydrospheric Processes.

Koster, R. D., Guo, Z., Yang, R., Dirmeyer, P. A., Mitchell, K., & Puma, M. J. (2009). On the nature of soil moisture in land surface models. Journal of Climate, 22(16), 4322-4335.

Kostov, K. G., & Jackson, T. J. (1993, April). Estimating profile soil moisture from surface layer measurements–A review. In *SPIE* (Vol. 1941, pp. 125-136).

Kumar, S. V., Reichle, R. H., Harrison, K. W., Peters-Lidard, C. D., Yatheendradas, S., & Santanello, J. A. (2012). A comparison of methods for a priori bias correction in soil moisture data assimilation. Water Resources Research, 48(3).

Lahoz, W. A., & De Lannoy, G. J. (2014). Closing the gaps in our knowledge of the hydrological cycle over land: conceptual problems. Surveys in Geophysics, 35(3), 623-660.

Leroux, D. J., Kerr, Y. H., Richaume, P., & Fieuzal, R. (2013). Spatial distribution and possible sources of SMOS errors at the global scale. Remote Sensing of Environment, 133, 240-250.

Lohmann, D., Nolte-Holube, R. and Raschke, E. (1996). A large scale horizontal routing model to be coupled to land surface parameterization schemes. Tellus 48A:708–721

Liang, X., & Xie, Z. (2001). A new surface runoff parameterization with subgrid-scale soil heterogeneity for land surface models. Advances in Water Resources, 24(9), 1173-1193.

Liang, X., Lettenmaier, D. P., Wood, E. F., & Burges, S. J. (1994). A simple hydrologically based model of land surface water and energy fluxes for general circulation models. Journal of Geophysical Research: Atmospheres, 99(D7), 14415-14428.

Liang, X., Wood, E. F., & Lettenmaier, D. P. (1996). Surface soil moisture parameterization of the VIC-2L model: Evaluation and modification. Global and Planetary Change, 13(1-4), 195-206.

Liang, X., Wood, E. F., & Lettenmaier, D. P. (1999). Modeling ground heat flux in land surface parameterization schemes. Journal of Geophysical Research: Atmospheres, 104(D8), 9581-9600.

Lievens, H., De Lannoy, G. J. M., Al Bitar, A., Drusch, M., Dumedah, G., Franssen, H. J. H., & Pan, M. (2016).Assimilation of SMOS soil moisture and brightness temperature products into a land surface model. Remote Sensing of Environment, 180, 292-304.

Lievens, H., Tomer, S. K., Al Bitar, A., De Lannoy, G. J. M., Drusch, M., Dumedah, G.,& Roundy, J. K. (2015). SMOS soil moisture assimilation for improved hydrologic simulation in the Murray Darling Basin, Australia. Remote Sensing of Environment, 168, 146-162.

Lohmann, D., NOLTE-HOLUBE, R. A. L. P. H., & Raschke, E. (1996).A large-scale horizontal routing model to be coupled to land surface parametrization schemes. Tellus A, 48(5), 708-721.

Martens, B., Lievens, H., Colliander, A., Jackson, T. J., & Verhoest, N. E. (2015). Estimating effective roughness parameters of the L-MEB model for soil moisture retrieval using passive microwave observations from SMAPVEX12. IEEE transactions on geoscience and remote sensing, 53(7), 4091-4103.

Matgen, P., Fenicia, F., Heitz, S., Plaza, D., de Keyser, R., Pauwels, V. R.,& Savenije, H. (2012). Can ASCAT-derived soil wetness indices reduce predictive uncertainty in well-gauged areas? A comparison with in situ observed soil moisture in an assimilation application. Advances in Water Resources, 44, 49-65.

Maurer, E. P., O'Donnell, G. M., Lettenmaier, D. P., & Roads, J. O. (2001). Evaluation of the land surface water budget in NCEP/NCAR and NCEP/DOE reanalyses using an off-line hydrologic model. Journal of Geophysical Research: Atmospheres, 106(D16), 17841-17862.

Merlin, O., Al Bitar, A., Walker, J. P., & Kerr, Y. (2010). An improved algorithm for disaggregating microwave-derived soil moisture based on red, near-infrared and thermal-infrared data. Remote Sensing of Environment, 114(10), 2305-2316.

Mohanty, B. P., Cosh, M. H., Lakshmi, V., & Montzka, C. (2017). Soil moisture remote sensing: State-of-the-science. Vadose Zone Journal, 16(1).

Narayan, U., Lakshmi, V., & Njoku, E. G. (2004). Retrieval of soil moisture from passive and active L/S band sensor (PALS) observations during the Soil Moisture Experiment in 2002 (SMEX02). Remote Sensing of Environment, 92(4), 483-496.

Nash, J. E., & Sutcliffe, J. V. (1970). River flow forecasting through conceptual models part I—A discussion of principles. Journal of hydrology, 10(3), 282-290.

Nijssen, B., Schnur, R., & Lettenmaier, D. P. (2001). Global retrospective estimation of soil moisture using the variable infiltration capacity land surface model, 1980–93. Journal of Climate, 14(8), 1790-1808.

Nikam, B.R., Garg, V., Gupta, P.K., Aggarwal, S.P., Srivastav, S.K.,& Senthil Kumar, A. (2017). Water availability in Ganga basin under changing LULC and climate. In International Conference on the Status and Future of the World's Large Rivers, organized at New Delhi, India, April 18-21, 2017.

Nikam, V.V., Nikam, B.R., Garg, V. & Aggarwal, S.P. (2015). Assimilation of remote Sensing derived soil moisture in macroscale hydrological model. In Proceedings of 'Hydro International 2015', 20th International Conference on Hydraulics, Water Resources and River Engineering organized at IIT Roorkee, India, 17-19 December, 2015.

Panciera, R., Walker, J. P., & Merlin, O. (2009). Improved understanding of soil surface roughness parameterization for L-band passive microwave soil moisture retrieval. IEEE Geoscience and Remote Sensing Letters, 6(4), 625-629.

Parrens, M., Calvet, J. C., de Rosnay, P., & Decharme, B. (2014). Benchmarking of L-band soil microwave emission models. Remote sensing of environment, 140, 407-419.

Pauwels, V. R., Hoeben, R., Verhoest, N. E., & De Troch, F. P. (2001). The importance of the spatial patterns of remotely sensed soil moisture in the improvement of discharge predictions for small-scale basins through data assimilation. Journal of Hydrology, 251(1), 88-102.

Pauwels, V., Hoeben, R., Verhoest, N. E., De Troch, F. P., & Troch, P. A. (2002). Improvement of TOPLATS-based discharge predictions through assimilation of ERS-based remotely sensed soil moisture values. Hydrological Processes, 16(5), 995-1013.

Rahmoune, R., Ferrazzoli, P., Kerr, Y. H., & Richaume, P. (2013). SMOS level 2 retrieval algorithm over forests: Description and generation of global maps. IEEE Journal of Selected Topics in Applied Earth Observations and Remote Sensing, 6(3), 1430-1439.

Rao, P. G. (1993). Climatic changes and trends over a major river basin in India. Climate Research, 215-223.

Reichle, R. H., & Koster, R. D. (2004). Bias reduction in short records of satellite soil moisture. Geophysical Research Letters, 31(19).

Sabater, J. M., De Rosnay, P., & Balsamo, G. (2011). Sensitivity of L-band NWP forward modelling to soil roughness. International journal of remote sensing, 32(19), 5607-5620.

Sahoo, A. K., De Lannoy, G. J., Reichle, R. H., & Houser, P. R. (2013). Assimilation and downscaling of satellite observed soil moisture over the Little River Experimental Watershed in Georgia, USA. Advances in water resources, 52, 19-33.

Sheffield, J., & Wood, E. F. (2008). Global trends and variability in soil moisture and drought characteristics, 1950–2000, from observation-driven simulations of the terrestrial hydrologic cycle. Journal of Climate, 21(3), 432-458.

Sheffield, J., Pan, M., Wood, E. F., Mitchell, K. E., Houser, P. R., Schaake, J. C., & Luo, L. (2003). Snow process modeling in the North American Land Data Assimilation System (NLDAS): 1. Evaluation of model-simulated snow cover extent. Journal of Geophysical Research: Atmospheres, 108(D22).

Shiradhonkar, S., Garg, V., Nikam, B. R., Thakur, P. K.,& Aggarwal, S. P. (2015). Hydrological Modelling of a Large River Basin Using Geospatial Tools. In Proceedings of 'Hydro International 2015', 20th International Conference on Hydraulics, Water Resources and River Engineering organized at IIT Roorkee, India, 17-19 December, 2015.

Todini, E. (1996). The ARNO rainfall—runoff model. Journal of hydrology, 175(1-4), 339-382.

Verhoest, N. E., van den Berg, M. J., Martens, B., Lievens, H., Wood, E. F., Pan, M., & Vernieuwe, H. (2015). Copula-based downscaling of coarse-scale soil moisture observations with implicit bias correction. *IEEE Transactions on Geoscience and Remote Sensing*, *53*(6), 3507-3521.

Walker, J. P., Willgoose, G. R., & Kalma, J. D. (2001). One-dimensional soil moisture profile retrieval by assimilation of near-surface measurements: A simplified soil moisture model and field application. Journal of Hydrometeorology, 2(4), 356-373.

Wang, J. R., O'Neill, P. E., Jackson, T. J., & Engman, E. T. (1983). Multifrequency measurements of the effects of soil moisture, soil texture, and surface roughness. IEEE Transactions on Geoscience and Remote Sensing, (1), 44-51.

Wigneron, J. P., Pardé, M., Waldteufel, P., Chanzy, A., Kerr, Y., Schmidl, S., & Skou, N. (2004). Characterizing the dependence of vegetation model parameters on crop structure, incidence angle, and polarization at L-band. IEEE Transactions on Geoscience and Remote Sensing, 42(2), 416-425.

Wood, E. F., Roundy, J. K., Troy, T. J., Van Beek, L. P. H., Bierkens, M. F., Blyth, E., Gochis, D., et al. (2011). Hyperresolution global land surface modeling: Meeting a grand challenge for monitoring Earth's terrestrial water. Water Resources Research, 47(5).

Xie, Z., Yuan, F., Duan, Q., Zheng, J., Liang, M., & Chen, F. (2007). Regional parameter estimation of the VIC land surface model: methodology and application to river basins in China. Journal of Hydrometeorology, 8(3), 447-468.

Zhao, R. -J., Zang, Y. -L., Fang, L. -R., Liu, X. -R., & Zhang, Q. -S. (1980). The Xinanjiang model. Hydrological Forecasting Proceedings Oxford Symposium, lASH. 129. (pp. 351–356).

Zhenghui, X., Fengge, S., Xu, L., Qingcun, Z., Zhenchun, H., & Yufu, G. (2003). Applications of a surface runoff model with Horton and Dunne runoff for VIC. Advances in Atmospheric Sciences, 20(2), 165-172.